Supporting Information for

Ultrasensitive Isothermal Detection of SARS-CoV-2 Based on Self-Priming Hairpin-Utilized Amplification of the G-Rich Sequence

Yan Li[†], Hansol Kim[†], Yong Ju[†], Yeonkyung Park[†], Taejoon Kang[‡, §], Dongeun Yong[//], and Hyun Gyu Park*[, †]

[†]Department of Chemical and Biomolecular Engineering (BK21 Four), Korea Advanced Institute of Science and Technology (KAIST), 291 Daehak-ro, Yuseong-gu, Daejeon 34141, Republic of Korea

[‡]Bionanotechnology Research Center, Korea Research Institute of Bioscience and Biotechnology (KRIBB), Yuseong-gu, Daejeon 34141, Republic of Korea

[§]School of Pharmacy, Sungkyunkwan University, 2066 Seobu-ro, Jangan-gu, Suwon, Gyeonggi-do 16419, Republic of Korea

[//]Department of Laboratory Medicine and Research Institute of Bacterial Resistance, Yonsei University College of Medicine, Seoul 03722, Republic of Korea

***Correspondence:**

Hyun Gyu Park Ph.D., Department of Chemical and Biomolecular Engineering (BK21 Four), KAIST, 291 Daehak-ro, Yuseong-gu, Daejeon 34141, Republic of Korea, Tel.: +82 42-350-3932, Fax: +82 42-350-3910, E-mail: hgpark@kaist.ac.kr

Table S1. Oligonucleotide Sequences Employed in This Work.

oligonucleotide name	sequence (5' → 3')
target RNA	GAC CCC AAA AUC AGC GAA AUG CAC CCC GCA UUA CGU UUG G
HP[a]	TCC CTC CCT CCC TCC CAG GGA CGA CTC TTT AAT TTA *CCA AAC GTA ATG CGG GGT GCA TTT CGC TGA TTT TGG GGT* CAT TAC GTT TGG TAA ATT AAA CCA AAC
G-rich sequence	CTG GGA GGG AGG GAG GGA

[a]Blue, orange, red, and purple letters in HP represent G-rich sequence template, nicking endonuclease recognition site, self-priming domain, and loop of self-primed hairpin, respectively. Italic letters in HP represent the target binding region.

Table S2. Clinical Specimen Analysis with qRT-PCR.

patient number	sample type	qRT-PCR		patient number	sample type	qRT-PCR	
		N gene	Result			N gene	Result
1	NPS[a]	+	Positive	51	Sputum	+	Positive
2	NPS	+	Positive	52	Sputum	+	Positive
3	NPS	+	Positive	53	NPS	+	Positive
4	NPS	+	Positive	54	NPS	+	Positive
5	NPS	+	Positive	55	NPS	+	Positive
6	NPS	+	Positive	56	NPS	+	Positive
7	NPS	+	Positive	57	Sputum	+	Positive
8	Sputum	+	Positive	58	Sputum	+	Positive
9	Sputum	+	Positive	59	NPS	+	Positive
10	Sputum	+	Positive	60	NPS	+	Positive
11	NPS	+	Positive	61	NPS	+	Positive
12	Sputum	+	Positive	62	Sputum	+	Positive
13	NPS	+	Positive	63	Sputum	+	Positive
14	Sputum	+	Positive	64	Sputum	+	Positive
15	NPS	+	Positive	65	Sputum	+	Positive
16	Sputum	+	Positive	66	Sputum	+	Positive
17	Sputum	+	Positive	67	Sputum	+	Positive
18	Sputum	+	Positive	68	Sputum	+	Positive
19	Sputum	+	Positive	69	Sputum	–	Negative
20	Sputum	+	Positive	70	Sputum	–	Negative
21	NPS	+	Positive	71	Sputum	–	Negative
22	Sputum	+	Positive	72	Sputum	–	Negative
23	Sputum	+	Positive	73	Sputum	–	Negative
24	NPS	+	Positive	74	Sputum	–	Negative
25	NPS	+	Positive	75	Sputum	–	Negative
26	NPS	+	Positive	76	Sputum	–	Negative
27	NPS	+	Positive	77	Sputum	–	Negative
28	NPS	+	Positive	78	NPS	–	Negative
29	NPS	+	Positive	79	Sputum	–	Negative
30	NPS	+	Positive	80	NPS	–	Negative
31	NPS	+	Positive	81	NPS	–	Negative

32	NPS	+	Positive	82	Sputum	–	Negative
33	NPS	+	Positive	83	Sputum	–	Negative
34	NPS	+	Positive	84	Sputum	–	Negative
35	NPS	+	Positive	85	Sputum	–	Negative
36	NPS	+	Positive	86	NPS	–	Negative
37	NPS	+	Positive	87	Sputum	–	Negative
38	NPS	+	Positive	88	Sputum	–	Negative
39	NPS	+	Positive	89	Sputum	–	Negative
40	NPS	+	Positive	90	Sputum	–	Negative
41	NPS	+	Positive	91	NPS	–	Negative
42	NPS	+	Positive	92	Sputum	–	Negative
43	NPS	+	Positive	93	Sputum	–	Negative
44	NPS	+	Positive	94	Sputum	–	Negative
45	NPS	+	Positive	95	NPS	–	Negative
46	NPS	+	Positive	96	Sputum	–	Negative
47	NPS	+	Positive	97	Sputum	–	Negative
48	NPS	+	Positive	98	NPS	–	Negative
49	NPS	+	Positive	99	NPS	–	Negative
50	Sputum	+	Positive	100	Sputum	–	Negative

[a]NPS represents nasopharyngeal swab

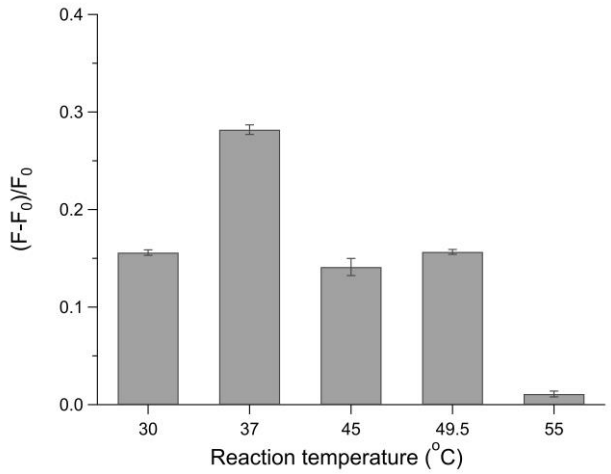

Figure S1. Optimization of reaction temperature in the presence of 1 nM target RNA. The fluorescence enhancement is defined as $(F - F_0)/F_0$, where F_0 and F are the fluorescence intensities at 496 nm in the absence and presence of target RNA, respectively. The final concentrations of HP, ThermoPol reaction buffer, NEBuffer 3.1, Bst, and Nt.BstNBI are 25 nM, 0.5X, 0.75X, 0.08 U/μL, and 0.08 U/μL, respectively. In this study, synthetic 40-mer RNA (Table S1) was used as target RNA. Error bars were calculated from triplicate experiments.

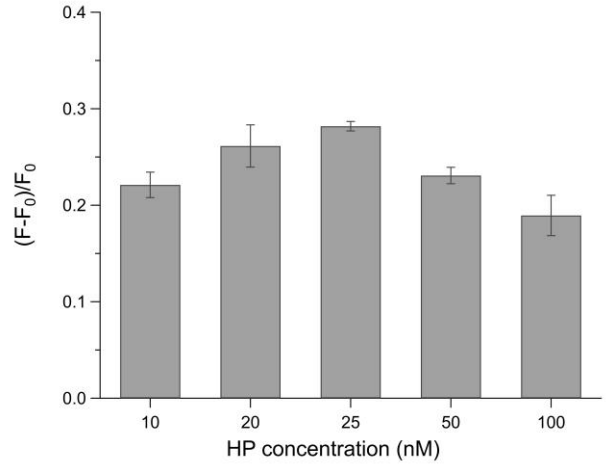

Figure S2. Optimization of HP concentration in the presence of 1 nM target RNA at 37 °C. The fluorescence enhancement is defined as $(F - F_0)/F_0$, where F_0 and F are the fluorescence intensities at 496 nm in the absence and presence of target RNA, respectively. The final concentrations of ThermoPol reaction buffer, NEBuffer 3.1, Bst, and Nt.BstNBI are 0.5X, 0.75X, 0.08 U/μL, and 0.08 U/μL, respectively. In this study, synthetic 40-mer RNA (Table S1) was used as target RNA. Error bars were calculated from triplicate experiments.

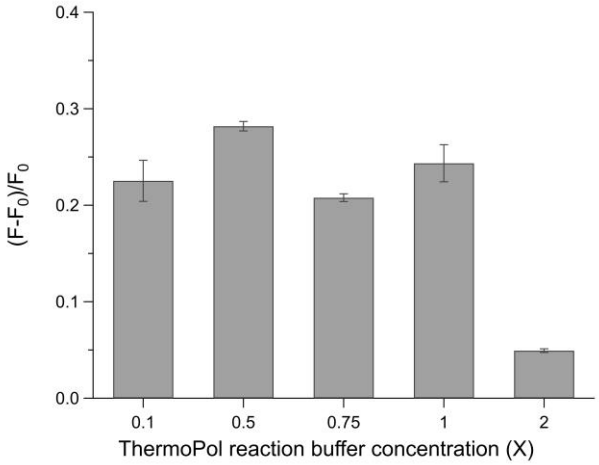

Figure S3. Optimization of ThermoPol reaction buffer concentration in the presence of 1 nM target RNA at 37 °C. The fluorescence enhancement is defined as $(F - F_0)/F_0$, where F_0 and F are the fluorescence intensities at 496 nm in the absence and presence of target RNA, respectively. The final concentrations of HP, NEBuffer 3.1, Bst, and Nt.BstNBI are 25 nM, 0.75X, 0.08 U/μL, and 0.08 U/μL, respectively. In this study, synthetic 40-mer RNA (Table S1) was used as target RNA. Error bars were calculated from triplicate experiments.

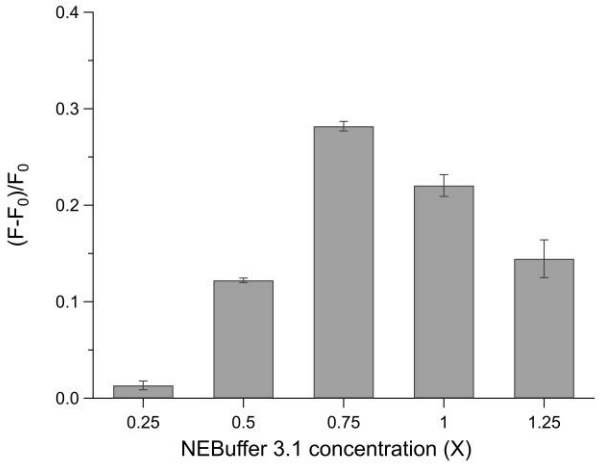

Figure S4. Optimization of NEBuffer 3.1 concentration in the presence of 1 nM target RNA at 37 °C. The fluorescence enhancement is defined as $(F - F_0)/F_0$, where F_0 and F are the fluorescence intensities at 496 nm in the absence and presence of target RNA, respectively. The final concentrations of HP, ThermoPol reaction buffer, Bst, and Nt.BstNBI are 25 nM, 0.5X, 0.08 U/μL, and 0.08 U/μL, respectively. In this study, synthetic 40-mer RNA (Table S1) was used as target RNA. Error bars

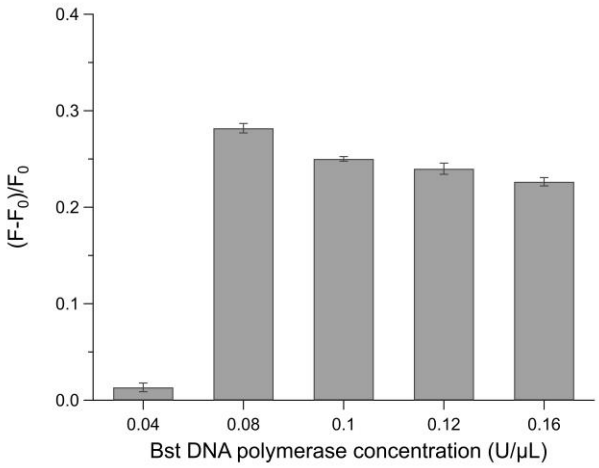

Figure S5. Optimization of Bst DNA polymerase concentration in the presence of 1 nM target RNA at 37 °C. The fluorescence enhancement is defined as $(F - F_0)/F_0$, where F_0 and F are the fluorescence intensities at 496 nm in the absence and presence of target RNA, respectively. The final concentrations of HP, ThermoPol reaction buffer, NEBuffer 3.1, and Nt.BstNBI are 25 nM, 0.5X, 0.75X, and 0.08 U/μL, respectively. In this study, synthetic 40-mer RNA (Table S1) was used as target RNA. Error bars were calculated from triplicate experiments.

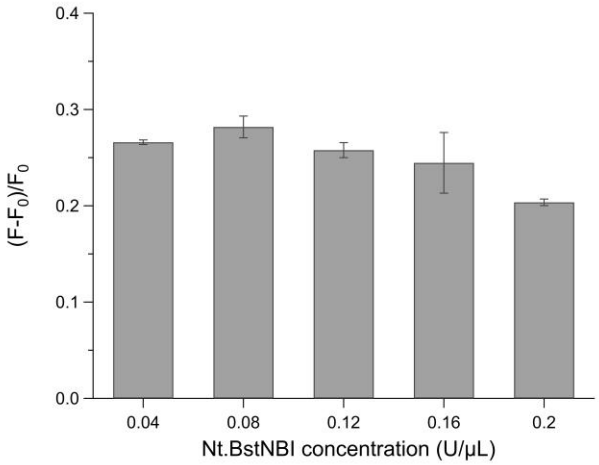

Figure S6. Optimization of Nt.BstNBI concentration in the presence of 1 nM target RNA at 37 °C. The fluorescence enhancement is defined as $(F - F_0)/F_0$, where F_0 and F are the fluorescence intensities at 496 nm in the absence and presence of target RNA, respectively. The final concentrations of HP, ThermoPol reaction buffer, NEBuffer 3.1, and Bst are 25 nM, 0.5X, 0.75X, and 0.08 U/μL, respectively. In this study, synthetic 40-mer RNA (Table S1) was used as target RNA. Error bars were calculated from triplicate experiments.

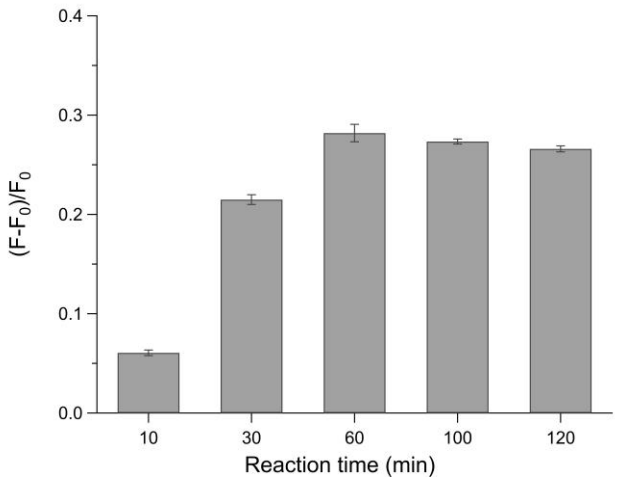

Figure S7. Optimization of reaction time in the presence of 1 nM target RNA at 37 °C. The fluorescence enhancement is defined as $(F - F_0)/F_0$, where F_0 and F are the fluorescence intensities at 496 nm in the absence and presence of target RNA, respectively. The final concentrations of HP, ThermoPol reaction buffer, NEBuffer 3.1, Bst, and Nt.BstNBI are 25 nM, 0.5X, 0.75X, 0.08 U/μL, and 0.08 U/μL, respectively. In this study, synthetic 40-mer RNA (Table S1) was used as target RNA. Error bars were calculated from triplicate experiments.